Contactless Palmprint Recognition Using Discriminant Multi-directional Feature Codes

Hoang Thien Van(✉)

Faculty of Information Technology, HUTECH University, Ho Chi Minh City, Vietnam
vt.hoang@hutech.edu.vn

Abstract. Contactless palmprint recognition attracts researchers due to challenges stemming from pose and illumination, impacting palm line layouts and visibility. This paper introduces a robust technique, Discriminant Multi-Directional Feature Codes (DMDFC), for contactless palmprint recognition. DMDFC features compute the Multi-Directional Feature Pattern (MDFP), which includes information about the clearest and second clearest ridges, along with the count of ridges passing through the examined point. Moreover, DMDFC segregates ridge and wrinkle features using the MDFP of the Negative Ridge Direction Image (NRDI) and the MDFP of the Positive Ridge Direction Image (PRDI). These MDFP maps undergo $(2D)^2$LDA for dimensionality reduction, resulting in highly discriminative features. Experimental evaluations using public datasets from PolyU and IITD demonstrate the superior accuracy of the proposed approach, indicating substantial progress in contactless palmprint recognition across diverse applications.

Keywords: Contactless palmprint · Gabor filters · multi directional code · 2DLDA · Recognition

1 Introduction

The rapid progress of modern civilization has spurred the demand for efficient technologies, particularly in security and privacy. Biometrics, dedicated to the study of human physiological and behavioral traits for individual authentication, encompasses various features, including signatures, gaits, voices, faces, fingerprints, and palmprints. Palmprint recognition stands out among these biometric methods due to its capacity to provide rich distinguishing information, such as principal lines, wrinkles, and texture [1]. Significantly, contactless palmprint recognition is an emerging field offering attractive solutions. It addresses hygiene concerns while enhancing user convenience and security. Researchers are actively developing contactless palmprint systems to improve user-friendliness and privacy protection. Nonetheless, contactless palmprint recognition presents its own set of challenges [2–6]. Unlike contact-based palmprint images, contactless images exhibit greater variability in scale, rotation, translation, and illumination. This

N.-S. Vo et al. (Eds.): INISCOM 2024, LNICST 595, pp. 169–180, 2024.
https://doi.org/10.1007/978-3-031-67357-3_12

variability increases intra class variations and may reduce recognition accuracy, necessitating advanced techniques to enhance contactless palmprint recognition accuracy. Palmprint recognition consists of three core stages: ROI segmentation, feature extraction, and matching. During ROI segmentation, a central palm subregion is singled out for its discriminative information [1,7]. In the palmprint extraction stage, recent biometric recognition methods for touchless images prioritize robust local texture descriptors capable of handling variations in scale, rotation, translation, and illumination [2]. These approaches fall into four categories: single direction based methods, local direction statistics based methods, and discriminant feature learning based methods [8–21]. The single direction based technique usually employs a specialized filter to detect and encode lines in a predetermined direction. Kong et al. [8] compute Gabor filters for encoding palmprint feature. Kong et al. [9] computed CompCode by applying six Gabor filters with different directions to detect the dominant direction of palm lines. Jie et al. [10] uses twelve Radon-based filters to compute the Robust Line Orientation Code (RLOC). Sun et al. [11] use three orthogonal Gaussian filters to calculate three orthogonal direction codes for feature extraction. Zhang et al. [13] introduce BOCV, which offers greater resistance to image rotation and provides an accurate depiction of local direction features. Fei et al. compute a neighbor direction descriptor to encode the six directions, which remains unaffected by noise or rotation [14]. Local direction statistics based methods compute encoded vectors derived from the statistics of direction patterns. Jia et al. suggest the use of the histogram of oriented lines (HOL) for palmprint recognition, which is robust against slight rotations and translations [15]. Luo et al. introduce the LLDP feature for palmprint recognition, encoding two dominant directions from palm lines [16]. Fei et al. [17] introduce LMDP feature to precisely capture information associated with multiple directions. Li et al. [18] propose LMTrP feature for palmprint recognition, utilizing local region histograms and kernel linear discriminant analysis to reduce dimensionality and eliminate redundant features. Zhang et al. present a collaborative representation (CR)-based approach, constructing feature vectors using blockwise histograms of competing codes [19]. Fei et al. [20] use convolutions between direction-based templates and palmprint images to create informative difference vectors, referred to as the DDBC code. In recent years, researchers have concentrated on developing discriminant feature learning based techniques, including subspace learning [21], metric learning [22,23], and deep learning [3,24–26], to establish mapping functions that transform palmprint images into discriminative feature subspaces. Chai et al. illustrate the effectiveness of a CNN model for both palmprint identification and gender classification [24]. Genovese et al. introduce PalmNet, a novel CNN integrated with Gabor filters, aiming for high recognition accuracy with touchless palmprint samples [25]. Liu et al. [26] use a fully convolutional network to generate deeply learned residual features for contactless palmprint identification. Ribaric et al. [21] introduce a multimodal biometric identification system that uses Principal Component Analysis (PCA) to extract discriminant palmprint features. Van et al. [27] proposed discriminant descriptors for palmprint

recognition by applying 2DLDA to positive and negative direction matrices. Rida et al. [28] introduce an ensemble classifier for palmprint recog-nition using the Random Subspace Method. Van et al. propose the Learning Discriminant Line Direction Descriptor (LDLDD), which independently learns all three types of directional pattern codes of palm lines [29]. This paper presents a robust algorithm, Discriminant Multi-Directional Feature Codes (DMDFC), designed for improving contactless palmprint recognition. The proposed method involves three key steps: (1) Applying Gabor filters at each pixel to assess ridges in eight different directions. (2) Computing the Multi-Directional Feature Pattern (MDFP), which provides details about the clearest and second clearest ridges, along with the count of ridges passing through the examined point. Additionally, it separates ridge and wrinkle features using the MDFP of the Negative Ridge Direction Image (NRDI) and the MDFP of the Positive Ridge Direction Image (PRDI). (3) projecting these MDFP maps to $(2D)^2$LDA for dimensionality reduction, resulting in highly discriminative features. Experimental results on the public datasets PolyU and IITD demonstrate the superior accuracy of the proposed DMDFC approach for contactless palmprint recognition. The article is structured as follows: Sect. 2 presents in detail our method, Sect. 3 shows experimental results, and Sect. 4 presents conclusions.

2 Discriminant Multi-directional Feature Codes

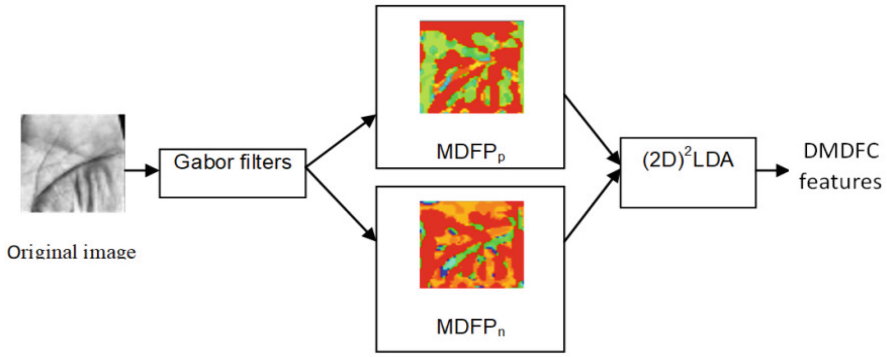

Fig. 1. The Framework of the Proposed Method

The characteristics of palm prints are defined by the patterns created by ridges and wrinkles. Since each pixel can contain multiple ridges or wrinkles, it is crucial to represent features that capture this complexity. To tackle this challenge, we introduce a multi-directional template that incorporates information about the clearest ridge, the second clearest ridge, and the count of ridges passing through the currently examined point. We employ Gabor filters to evaluate the ridges in eight different directions. The outcomes of these filters are

utilized to identify the clearest ridge, the second clearest ridge, and to compute the number of ridges at the examined point. Ridges and wrinkles often have opposite directions. To avoid confusion in matching directional pattern features, we segregate these two types of pixels into two distinct images: one containing pixels with the clearest lines in the positive direction (angle > 0) and another containing pixels with the clearest lines in the negative direction (angle $<= 0$). To generate distinctive and compact features, we apply 2D2LDA to the images of negative ridge direction and positive ridge direction. The outcome is a discriminant multi-directional feature code for classification employing the Normalized Squared Euclidean distance. Figure 1 illustrates the processing steps of our proposed method.

2.1 Multi-directional Feature Pattern

We propose a multi-directional feature template, which comprises two distinct images: the Negative Ridge Direction Image (NRDI) and the Positive Ridge Direction Image (PRDI) for representing distinct ridges and wrinkles. PRDI contains multi-directional patterns of the clearest lines in the positive direction (angle > 0), while NRDI contains multi-directional patterns of the clearest lines in the negative direction (angle $<= 0$). This template includes information about the clearest ridge, the second clearest ridge, and the count of ridges passing through the currently examined point. We utilize Gabor filters to identify the clearest ridge, the second clearest ridge, and calculate the number of ridges at the examined point. Additionally, we use the Dominant Direction Number (DDN) [17] to compute the number of ridges. MDFT is defined as follows:

$$mdfp_p = \begin{cases} \left(m_f \times {N_\theta}^2 + DDN \times N_\theta + m_s\right) \ if\ \theta_{mf} > 0 \\ 0\ otherwise \end{cases} \tag{1}$$

$$mdfp_n = \begin{cases} \left(m_f \times {N_\theta}^2 + DDN \times N_\theta + m_s\right) \ if\ \theta_{mf} \leq 0 \\ 0\ otherwisD \end{cases} \tag{2}$$

$$DDN = \frac{1}{2}\sum_{j=1}^{N_\theta} \left| s\left(r_j - r_{\varphi(j)}\right) - s\left(r_{\varphi(j)} - r_{\varphi(\varphi(j))}\right)\right| \tag{3}$$

$$\varphi\left(j\right) = mod\left(j-2, N_\theta\right) + 1 \tag{4}$$

$$r_j = \left(I * G\left(\theta_j\right)\right)_{(x,y)} \tag{5}$$

$\theta_j = \frac{\pi(j-1)}{n} j = 1, 2, \ldots, N_\theta$ GrindEQ$_6$

where m_f and m_s represents the indices of the directions with the minimum and the second-minimum filtering response, respectively. DDN is the number of the dominant directions. N_θ (with $N_\theta = 8$) stands for the total number of directions corresponding to Gabor functions. The variable j signifies the direction index, r_j signifies the result of Gabor convolution in the j-th direction, and $s(x)$ is a function that equals 1 if x is greater than 0, and 0 otherwise. $\varphi(j)$ represents the adjacent clockwise direction index to j, and it is defined as N_θ if $j = 1$, and (j

− 1) otherwise. I denotes the palmprint image. $G(\theta_j)$ represents the real part of the Gabor filter with orientation θ_j, '*' indicates the convolution operator, and *(x, y)* signifies the pixel's position in I. The 2D-Gabor filter [8] (Fig. 2) is computed using these formulas:

$$G\left(x,\ y,\ \theta, \mu, \sigma\right) = \frac{1}{2\pi\sigma^2} exp\left\{-\frac{x^2+y^2}{2\sigma^2}\right\} exp\left\{2\pi i(\mu x cos\theta\ + \mu y sin\theta)\ \right\} \quad (6)$$

In this context, μ is the frequency of the sinusoidal wave, i denotes the imaginary unit, θ is a parameter for direction determination, and σ represents the standard deviation of the Gaussian envelope.

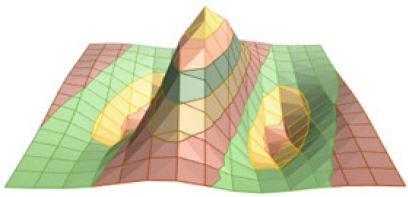

Fig. 2. Gabor filter

These matrices computed by the MDFP technique still possess large dimensions and contain redundant information. The following section will explain how $(2D)^2$LDA is used to extract discriminative features for classification.

2.2 $(2D)^2$LDA

$(2D)^2$LDA [29,30] refers to a two-directional 2DLDA. It entails applying 2DLDA to the row-wise direction of the input matrices to learn an optimal projection matrix Q and to the column-wise direction of the matrices to learn an optimal projection matrix Z by computing a set of optimal discriminating vectors $X_Q = \left\{x_Q^1,\ x_Q^2,\ \ldots,\ x_Q^d\right\}$ and $X_Z = \left\{x_z^1,\ x_z^2,\ \ldots,\ x_z^t\right\}$ by maximizing the 2D Fisher criterion $J_Q\left(X\right)$ and $J_Z\left(X\right)$ defined as:

$$J_Q\left(X\right) = \frac{{X_Q}^T G_b X_Q}{{X_Q}^T G_w X_Q} \quad (7)$$

$$J_Z\left(X\right) = \frac{{X_Z}^T H_b X_Z}{{X_Z}^T H_w X_Z} \quad (8)$$

$$G_b = \frac{1}{N}\sum_{i=1}^{C} n_i \left(A_i - \overline{A}\right)\left(A_i - \overline{A}\right)^T \quad (9)$$

$$G_w = \frac{1}{N}\sum_{i=1}^{C}\sum_{j=1}^{n_i} \left(A_j - \overline{A_i}\right)\left(A_j - \overline{A_i}\right)^T \quad (10)$$

$$H_b = \frac{1}{N}\sum_{i=1}^{C} n_i \left(A_i^T - \overline{A^T}\right)\left(A_i^T - \overline{A^T}\right)^T \tag{11}$$

$$H_w = \frac{1}{N}\sum_{i=1}^{C}\sum_{j=1}^{n_i} \left(A_j^T - \overline{A_i^T}\right)\left(A_j^T - \overline{A_i^T}\right)^T \tag{12}$$

Consider a set of input matrices $\{A_k\}$, where k ranges from *1* to N, and these matrices belong to C distinct classes. Class C_i includes n_i samples (with $\sum_{i=1}^{C} n_i = N$). $\overline{A}$ represents the mean matrix across all classes, while $\overline{A}_i$ denotes the mean matrix of the *ith* class. The notation T indicates matrix transpose. In the row-wise direction, G_b and G_w denote the between-class and within-class scatter matrices, respectively. Similarly, in the column-wise direction, H_b and H_w fulfill the same roles as the between-class and within-class scatter matrices. Furthermore, d and t correspond to the chosen numbers of the largest eigen values of $G_w^{-1}G_b$ and $H_w^{-1}H_b$ respectively. The input matrix $A_{m\times n}$ is projected onto $Q_{n\times d}$ and $Z_{m\times q}$ simultaneously, yielding a feature matrix $Y_{q\times d}$ as follows:

$$Y = Z^T.A.Q \tag{13}$$

$(2D)^2$LDA offers the benefit of reducing feature dimensionality in both rows and columns while simultaneously generating highly discriminative features for distinguishing between classes. The next sub section will describe how $(2D)^2$LDA is applied to the NRDI and the PRDI to produce DMDFC features.

2.3 DMDFC for Palmprint Recognition

Initially, the Region of Interest (ROI) is identified [32], and serves as the input for our proposed method. The process for obtaining DMDFC features through our proposed method proceeds as follows:

1. Step 1: Applying eight Gabor filters to detect ridges or wrinkles in various directions using formulas (5), (6), (7).
2. Step 2: Computing the DNN feature based on the responses of the Gabor filters using formulas (3), (4).
3. Step 3: Calculating the NRDI matrix ($mdfp_p$) and the PRDI matrix ($mdfp_n$) using formulas (1), (2).
4. Step 4: Applying $(2D)^2$LDA to combine the matrix of $mdfp_p$ and $mdfp_n$ matrices using formulas (7)-(13), resulting in the feature matrix denoted as Y.

To classify a query image I, we compute the DMDFC feature Y. Subsequently, our method is applied to all N training images to acquire the DMDFC feature matrix Y_k (where k = 1, 2, ..., N). Following that, we utilize the nearest neighbor classifier for classification purposes. In this context, the distance between Y and Y_k is computed as follows: (Y, Y_k) = $\|Y - Y_k\|$. The distance (Y, Y_k) falls within the range of 0 to 1, with a perfect match having a distance of 0. Figure 3 shows DMDFC features.

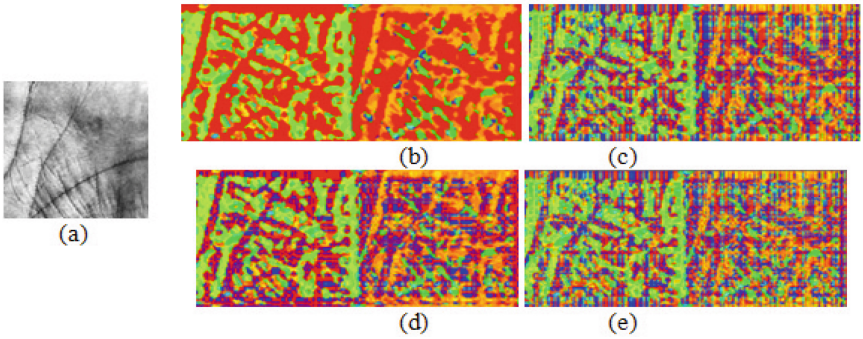

Fig. 3. Results of MDFP and $(2D)^2$LDA: (a) Original Image, (b) DMDFC Image, Reconstructed Images of the MDFP Image with: (c) (d = 100, q = 80), (d) (d = 80, q = 100), (e) (d = 80, q = 80).

3 Experimental Results

We performed experiments using widely utilized palmprint databases, specifically the Palmprint PolyU and IITD datasets. This involved conducting various tests and analyses on these datasets to evaluate the effectiveness of our approach. The PolyU palmprint database, known as the contact-free 3D/2D Hand Images Database, encompasses 1770 2D images gathered from 177 subjects [31]. For each subject, there are five images captured in different poses. The resolution of these images is 640×480 pixels. The algorithm outlined in [33] was used to align each palmprint image and extract an ROI with a size of 128×128 (Fig. 4a). The IITD palmprint database consists of 2601 palmprint images sourced from 460 distinct palms, encompassing 230 volunteers. Each volunteer contributed five or six palmprint images for both their left and right palms during the image collection phase. All individuals included in the database fall within the age range of 14 to 15 years. The dimensions of the provided Region of Interest (ROI) image are 150×150 pixels [33]. In our experimental setup, we employ Region of Interest (ROI) databases where each image is resized to 100×100 pixels to assess the performance of our feature extraction methods (Fig. 4). Table 1 presents information regarding the experimental parameters utilized for both the IITD and PolyU datasets. The algorithms were implemented in C# on a PC equipped with

Table 1. Experimental Dataset Parameters.

Data set	One class			All class		Number of distance scores	
	Train set	Test set		Train set	Test set		
		Reg.	Unreg.			Correct	Incorrect
IITD	2	3	3	$300(2 \times 150)$	$450(3 \times 150) + 150\ (3 \times 50) = 600$	450	600
PolyU	5	5	5	$750(5 \times 150)$	$750(5 \times 150) + 42\ (5 \times 27) = 885$	750	885

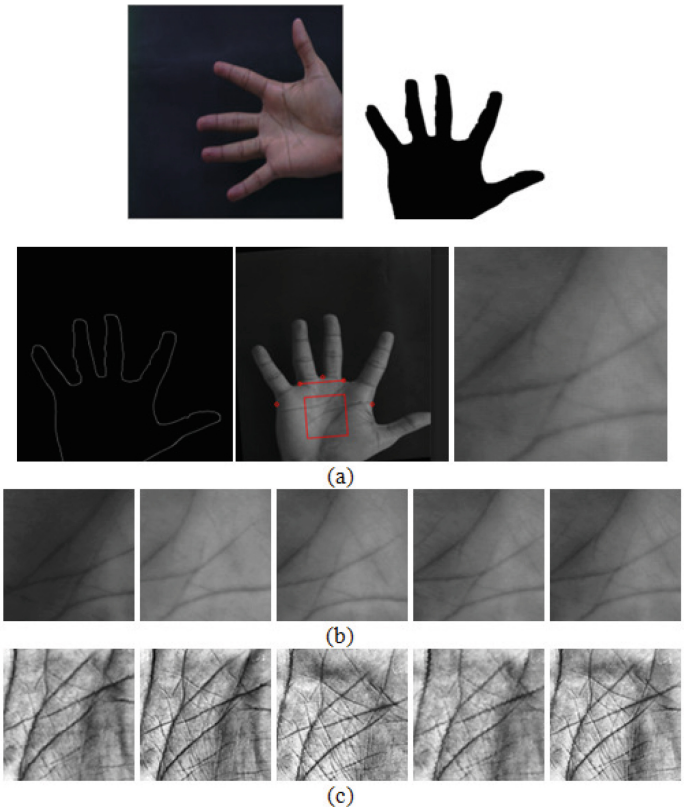

Fig. 4. Steps of ROI Extraction (a), Palmprint ROI samples from (b) PolyU, and (c) IITD databases.

an Intel(R) Core(TM) i5-9300U CPU @ 2.40 GHz and running the Windows 10 Professional operating system.

Palmprint identification involves matching a queried palmprint image against multiple templates to determine its class label. We assess identification accuracy using the rank-1 identification rate, wherein the query is compared against all training templates, and the label of the most similar template is assigned as the class label for the query. Verification, on the other hand, verifies whether an individual is who they claim to be through one-to-one comparisons. To compute correct and incorrect distances, each query in the test set is compared against all templates in the training set. Correct distances for a query in the test set are obtained by matching it with corresponding samples in the training set, while incorrect distances are derived by comparing it to samples from other palms in the training set. Genuine acceptance is observed when the matching distance between samples from the same palm falls below the threshold, whereas false acceptance occurs when the matching distance between samples from different palms is below the threshold. The Equal Error Rate (EER) is computed from

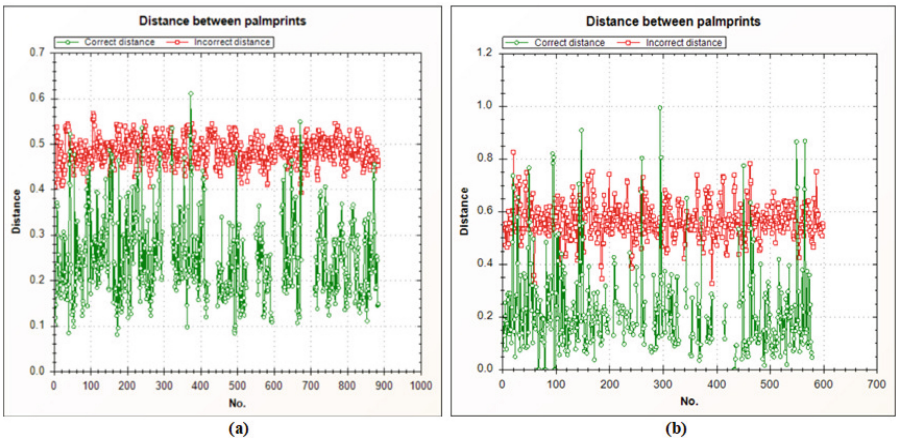

Fig. 5. Distribution of Matching Distances for Our Proposed Method on the (a) PolyU and (b) IITD Datasets, respectively.

Table 2. Performance results on the PolyU Dataset

Methods	EER	ACC (Rank-1)	Feature Extraction Time (s)
HOL [15]	3.39%	97.2%	0.025
LLDP [16]	2.71%	98.6%	0.063
PalmNet [25]	2.14%	99.2%	1.720
LDDBP [20]	1.69%	99.3%	0.085
Our method	1.35%	99.7%	0.426

the statistical pairs of False Reject Rate (FRR) and False Accept Rate (FAR). Figure 5 depicts the distribution of matching distances computed by our method across the IITD and PolyU datasets. Table 2 presents the performance results of our proposed method compared to state-of-the-art methods on the PolyU dataset, while Table 3 displays the performance on the IITD dataset. These results demonstrate that the proposed method achieves high accuracy on both the IITD and PolyU datasets.

Table 3. Performance results on the IITD Dataset.

Methods	EER	ACC (Rank-1)	Feature Extraction Time (s)
HOL [15]	7.20%	86.4%	0.031
LLDP [16]	5.83%	90.8%	0.072
Palmnet [25]	4.50%	91.1%	1.925
LDDBP [20]	4.33%	92.4%	0.092
Our method	3.16%	93.1%	0.525

4 Conclusion

Contactless palmprint recognition grapples with challenges posed by pose and illumination variations, impacting palm line layouts and visibility. The palmprint's directional information emerges as a promising feature for recognition. The introduction of the Discriminant Multi-Directional Feature Codes (DMDFC) technique in this paper offers a novel and effective solution. DMDFC, specifically the Multi-Directional Feature Pattern (MDFP), captures vital data about the clearest and second clearest ridges, as well as the count of ridges passing through each examined point. Notably, DMDFC adeptly separates ridge and wrinkle features via the MDFP of the Negative Ridge Direction Image (NRDI) and the MDFP of the Positive Ridge Direction Image (PRDI). Furthermore, the application of $(2D)^2$ LDA for dimensionality reduction on these MDFP maps yields highly discriminative features. Experimental assessments on public datasets PolyU and IITD unambiguously affirm the superior accuracy of the proposed DMDFC approach. In our future endeavors, we aim to enhance the method's robustness and extend its application to other biometric characteristics.

References

1. Kong, A., Zhang, D., Kamel, M.: A survey of palmprint recognition. Pattern Recogn. **42**(7), 1408–1418 (2009). https://doi.org/10.1016/j.patcog.2009.01.018. ISSN 0031-3203
2. Alausa, D.W.S., et al.: Contactless palmprint recognition system: a survey. IEEE Access **10**, 132483–132505 (2022). https://doi.org/10.1109/ACCESS.2022.3193382
3. Liang, X., Fan, D., Yang, J., Jia, W., Lu, G., Zhang, D.: PKLNet: keypoint localization neural network for touchless palmprint recognition based on edge-aware regression. IEEE J. Sel. Top. Sig. Process. **17**(3), 662–676 (2023). https://doi.org/10.1109/JSTSP.2023.3241540
4. Liang, X., Li, Z., Fan, D., Zhang, B., Lu, G., Zhang, D.: Innovative contactless palmprint recognition system based on dual-camera alignment. IEEE Trans. Syst. Man Cybern. Syst. **52**(10), 6464–6476 (2022). https://doi.org/10.1109/TSMC.2022.3146777

5. Yu, L., Yi, Q., Zhou, K.: Multi-scale discriminant representation for generic palmprint recognition. Neural Comput. Applic. **35**, 13147–13165 (2023). https://doi.org/10.1007/s00521-023-08355-w
6. Zhang, L., Li, L., Yang, A., Shen, Y., Yang, M.: Towards contactless palmprint recognition: a novel device, a new benchmark, and a collaborative representation based identification approach. Pattern Recogn. **69**, 199–212 (2017). https://doi.org/10.1016/j.patcog.2017.04.016. ISSN 0031-3203
7. Xiao, Q., Lu, J., Jia, W., Liu, X.: Extracting palmprint ROI from whole hand image using straight line clusters. IEEE Access **7**, 74327–74339 (2019). https://doi.org/10.1109/ACCESS.2019.2918778
8. Kong, W.K., Zhang, D., Li, W.: Palmprint feature extraction using 2-D Gabor filters. Pattern Recogn. **36**(10), 2339–2347 (2003). https://doi.org/10.1016/S0031-3203(03)00121-3. ISSN 0031-3203
9. Kong, A.W.K., Zhang, D.: Competitive coding scheme for palmprint verification. In: Proceedings 17th International Conference Pattern Recognition (ICPR), Cambridge, U.K., vol. 1, pp. 520–523 (2004). https://doi.org/10.1109/ICPR.2004.1334184
10. Jia, W., Huang, D., Zhang, D.: Palmprint verification based on robust line orientation code. Pattern Recogn. **41**(5), 1504–1513 (2008). https://doi.org/10.1016/j.patcog.2007.10.011
11. Sun, Z., Tan, T., Wang, Y., Li, S.Z.: Ordinal palmprint represention for personal identification. In: Proceedings IEEE Conference on Computer Vision and Pattern Recognition (CVPR), vol. 1, pp. 279–284 (2005). https://doi.org/10.1109/CVPR.2005.267
12. Guo, Z., Zhang, D., Zhang, L., Zuo, W.: Palmprint verification using binary orientation co-occurrence vector. Pattern Recogn. Lett. **30**(13), 1219–1227 (2009). https://doi.org/10.1016/j.patrec.2009.05.010
13. Zhang, L., Li, H., Niu, J.: Fragile bits in palmprint recognition. IEEE Sig. Process. Lett. **19**(10), 663–666 (2012). https://doi.org/10.1109/LSP.2012.2211589
14. Fei, L., Zhang, B., Xu, Y., Yan, L.: Palmprint recognition using neighboring direction indicator. IEEE Trans. Hum.-Mach. Syst. **46**(6), 787–798 (2016). https://doi.org/10.1109/THMS.2016.2586474
15. Jia, W., Hu, R.-X., Lei, Y.-K., Zhao, Y., Gui, J.: Histogram of oriented lines for palmprint recognition. IEEE Trans. Syst. Man Cybern. Syst. **44**(3), 385–395 (2014). https://doi.org/10.1109/TSMC.2013.2258010
16. Luo, Y.T., et al.: Local line directional pattern for palmprint recognition. Pattern Recogn. **50**, 26–44 (2016). https://doi.org/10.1016/j.patcog.2015.08.025
17. Fei, L., Wen, J., Zhang, Z., Yan, K., Zhong, Z.: Local multiple directional pattern of palmprint image. In: Proceedings 23rd International Conference Pattern Recognition (ICPR), pp. 3013–3018 (2016). https://doi.org/10.1109/ICPR.2016.7900096
18. Li, G., Kim, J.: Palmprint recognition with local micro-structure tetra pattern. Pattern Recogn. **61**, 29–46 (2017). https://doi.org/10.1016/j.patcog.2016.06.025
19. Fei, L., Zhang, B., Teng, S., Zhang, W.: Local apparent and latent direction extraction for palmprint recognition. Inf. Sci. **473**, 59–72 (2019). https://doi.org/10.1016/j.ins.2018.09.032
20. Fei, L., Zhang, B., Xu, Y., Huang, D., Jia, W., Wen, J.: Local discriminant direction binary pattern for palmprint representation and recognition. IEEE Trans. Circuits Syst. Video Technol. **30**(2), 468–481 (2020). https://doi.org/10.1109/TCSVT.2019.2890835

21. Ribaric, S., Fratric, I.: A biometric identification system based on Eigenpalm and Eigenfinger features. IEEE Trans. Pattern Anal. Mach. Intell. **27**(11), 1698–1709 (2005)
22. Wen, J., et al.: Robust sparse linear discriminant analysis. IEEE Trans. Circuits Syst. Video Technol., 1–13 (2018). https://doi.org/10.1109/TCSVT.2018.2799214
23. Lu, J., Liong, V.E., Zhou, X., Zhou, J.: Learning compact binary face descriptor for face recognition. IEEE Trans. Pattern Anal. Mach. Intelli. **37**(10), 2041–2056 (2015). https://doi.org/10.1109/TPAMI.2015.2408359
24. Chai, T., Prasad, S., Wang, S.: Boosting palmprint identification with gender information using DeepNet. Future Gener. Comput. Syst. **99**, 41–53 (2019). https://doi.org/10.1016/j.future.2019.04.013
25. Genovese, A., Piuri, V., Plataniotis, K.N., Scotti, F.: PalmNet: Gabor-PCA convolutional networks for touchless palmprint recognition. IEEE Trans. Inf. Forensics Secur. **14**(12), 3160–3174 (2019). https://doi.org/10.1109/TIFS.2019.2911165
26. Liu, Y., Kumar, A.: Contactless palmprint identification using deeply learned residual features. IEEE Trans. Biometrics Behav. Identity Sci. **2**(2), 172–181 (2020). https://doi.org/10.1109/TBIOM.2020.2967073
27. Van, H.T., Le, T.H.: On discriminant orientation extraction using GridLDA of line orientation maps for palmprint identification. In: Huynh, V., Denoeux, T., Tran, D., Le, A., Pham, S. (eds.) Knowledge and Systems Engineering. AISC, vol. 244, pp. 237–248. Springer, Cham (2014). https://doi.org/10.1007/978-3-319-02741-8_21
28. Rida, I., Herault, R., Marcialis, G., Gasso, G.: Palmprint recognition with an efficient data driven ensemble classifier. Pattern Recog. Lett., 1–7 (2018). https://doi.org/10.1016/j.patrec.2018.04.033
29. Van Thien, H., Phan, T.D.D., Le, T.H.: Palmprint recognition using learning discriminant line direction descriptors. In: Phan, C.V., Nguyen, T.D. (eds.) Nature of Computation and Communication. ICTCC 2022. LNICS, vol. 473, pp. 148–159. Springer, Cham (2022). https://doi.org/10.1007/978-3-031-28790-9_10
30. Noushath, S., Hemantha Kumar, G., Shivakumara, P.: $(2D)^2$LDA: an efficient approach for face recognition. Pattern Recogn. **39**(7), 1396–1400 (2006). https://doi.org/10.1016/j.patcog.2006.01.018
31. PolyU Palmprint Database: https://www4.comp.polyu.edu.hk/~csajaykr/myhome/database_request/3dhand/Hand3D.htm. Accessed 1 Nov 2023
32. IITD Touchless Palmprint Database: https://www4.comp.polyu.edu.hk/~csajaykr/IITD/Database_Palm.htm. Accessed 10 Nov 2023
33. Kumar, A.: Incorporating cohort information for reliable palmprint authentication. In: Proceedings 6th Indian Conference on Computer Vision, Graphics and Image Processing, Bhubaneswar, India, December 2008, pp. 583–590 (2008). https://doi.org/10.1109/ICVGIP.2008.73